Dall'Osto, M., Beddows, D. C. S., Kinnersley, R. P., Harrison, R. M., Donovan, R. J. and Heal, M. R. (2004) Characterisation of individual airborne particles by using aerosol time-of-flight mass spectrometry (ATOFMS) at Mace Head, Ireland, *J. Geophys. Res.* **109,** D21302

http://dx.doi.org/10.1029/2004JD004747

Characterization of individual airborne particles by using aerosol time-of-flight mass spectrometry at Mace Head, Ireland

Manuel Dall'Osto[1], David C. S. Beddows[1], Robert P. Kinnersley[1], Roy M. Harrison[1], Robert J. Donovan[2] and Mathew R. Heal[2]

[1]Division of Environmental Health and Risk Management, University of Birmingham, Birmingham, UK. [2]School of Chemistry, University of Edinburgh, Edinburgh, UK.

Abstract

[1] An aerosol time-of-flight mass spectrometer was deployed at Mace Head (Ireland) during August 2002. The measurements provide qualitative chemical composition and size distribution (0.3–3 μm) information for single particles. Three broad categories of particles: sea salt, dust, and carbon-containing particles were identified and apportioned, and their temporal evolution (1 hour resolution) is described. Aerosol sources were correlated with meteorological factors and with air mass trajectories, demonstrating long-range transport of different continental air masses from Europe, Africa, and America. The major class of particles was derived from sea salt and was subdivided into pure, mixed, and aged sea salt according to the extent of displacement of chloride by nitrate. Two types of dust particles were found mainly in the coarse mode (>1 μm); the former, thought to originate from the Sahara, presented an aluminium/silicon signature, while the latter, of more local origin, had a calcium-rich composition. Carbon-containing particles were mainly distributed in the fine mode (<1 μm) and associated with different chemical species in different size modes, suggesting different mechanisms of formation.

Keywords: ATOFMS, Mace Head, marine aerosols, Saharan dust, aerosol mass spectrometry.

1. Introduction

[2] Understanding the physical and chemical properties of marine aerosol particles is crucial because of the role these particles play in a number of atmospheric processes. Marine aerosols affect climate directly through scattering and absorption of radiation and indirectly as they can act as cloud condensation nuclei. In addition, marine aerosol particles play an important role in the cycling of various elements through the atmosphere [Heintzenberg et al., 2000].

[3] The majority of air masses arriving at Mace Head Atmospheric Research Station (53°19′N, 9°54′W), Galway, Ireland, arrive from the nominal clean sector [Jennings et al., 1993], which lies between compass bearings 180° and 300°, and are dominated by southwesterly winds from the Atlantic Ocean. Most of these air masses are considered clean (not strongly influenced by anthropogenic activity), and Mace Head is well suited for marine background experiments. However, air masses arriving from both inside and outside this clean sector carry influences of continental sources, i.e., North America and Europe [Jennings et al., 1997] as well as local land sources. Therefore, by studying aerosol at Mace Head, information on marine sources, emissions from

Europe, and long-range transport across the Ocean can be obtained. Studies of aerosol sources at Mace Head have been conducted as part of the Atmosphere/Ocean Chemistry Experiment (AEROCE). Daily aerosol samples were collected for almost 5 years, from 1989 to 1994, and compared with three other sites, Barbados, Bermuda, and Izana. It was found that Mace Head had the lowest dust concentrations but the highest sea-salt concentrations [Arimoto et al., 1995]. Huang et al. [2001], by using positive matrix factorization (PMF), were able to study the sources and source variations for aerosol at Mace Head. Six classes were apportioned: mineral dust, sea salt, general pollution, a secondary SO4-Se signal, ferrous industries, and a second (possibly biogenic) marine source. Recent estimates based on the continental nss-SO4/Sb mass ratio indicate that, on an annual basis, the contributions from anthropogenic sources account for about 85–90% of the total nss-SO42− in aerosols at Mace Head [Savoie et al., 2002]. More recently, as part of the "New Particle Formation and Fate in the Coastal Environment" (PARFORCE) study, a broad range of physical and chemical aerosol properties were measured in two intensive measurement campaigns [O'Dowd et al., 2002].

[4] During August and September 2002 the North Atlantic Marine Boundary Layer Experiment (NAMBLEX) took place at Mace Head. The aims of the campaign were to study the oxidation processes, atmospheric chemistry and composition of a number of species primarily in the marine boundary layer. As part of this campaign, an aerosol time-of-flight mass spectrometer (ATOFMS) was operated continuously for 3 weeks in August 2002. The ATOFMS allows for the characterization of the aerodynamic diameter and chemical composition of single particles from a polydisperse aerosol in real time. The purpose of this study was to characterize individual particles at a remote marine site. Data on particle size and a series of chemical markers were used to classify individual particles in the atmosphere according to their source and composition.

[5] Performing searches for different chemical markers, the ATOFMS can provide a qualitative picture of the trends in the number concentrations of a particular species with high time resolution, and assist in the source apportionment of aerosol at the remote marine site at Mace Head. The temporal profiles of different species obtained could be correlated with meteorological factors such as wind speed, wind direction, relative humidity, and air temperature to assess the relative influence of transport and local sources. In addition, air mass back trajectories were used to identify the atmospheric transport pathways to Mace Head, in order to provide information on the characteristics of different continental air masses.

2. Experimental Setup

[6] From 1–21 August 2002 (Julian days 213 to 233) an aerosol time-of-flight mass spectrometer (ATOFMS) was operated almost continuously at the Mace Head Atmospheric Research Station. The research station is located on the west coast of Ireland (53°19′N, 9°54′W) at close to sea level on a peninsula, which is surrounded by coastline and tidal areas except for a small sector between 20° and 40°. The nominal clean sector lies between 180° and 300° [Jennings et al., 1997]. The inlet of the instrument was linked by a stainless steel pipe (diameter and length 0.25 inch and 2 m, respectively) to a manifold connected to a 22 m 250 mm pumped down pipe attached to a sampling tower. The sampling height was alternated between 7 and 22 m

hourly by switching a valve in the pipe at 7 m height. Data analysis showed no significant difference in the particle populations sampled at the two heights.

2.1. ATOFMS

[7] The ATOFMS provides continuous, real-time detection and characterization of single particles from polydisperse samples, providing information on particle size and composition. The first instrument (a laboratory-based mass spectrometer) was built in 1993 [Prather et al., 1994] by K. A. Prather at the University of California (UCR), and the first transportable version was developed only a few years later [Gard et al., 1997]. In 1998, TSI Incorporated acquired the license to build the ATOFMS and developed the current Model 3800 used in this study. Since the design was not changed much, only a short description of the commercial version (TSI, Model 3800) will be presented here. Briefly, air is introduced into a vacuum system region through a converging nozzle. At this point, two differentially pumped regions separated by skimmers create a narrow collimated particle beam, which travels through a sizing region where the aerodynamic diameter of individual particles is determined. In order to obtain the particle aerodynamic diameter, the velocity of each particle is determined from the transit time between two continuous-wave laser beams situated a known distance apart. The scattered light signals caused by the particle passing through the two lasers (532 nm, diode-pumped solid state lasers) are detected using photomultiplier tubes (PMT). The velocity and the aerodynamic diameter of the particle are related by a calibration curve obtained using polystyrene latex sphere (PSL) suspensions of known size in the range between 0.3 and 2.4 μm.

[8] After being sized, the particles enter the mass spectrometer source region. Here a pulse from a Nd:YAG laser (frequency quadrupled, $\lambda = 266$ nm) is triggered at the appropriate time, based on the transit time of the particle measured in the sizing region, to desorb and ionize material from the sized particle. The mass-to-charge ratios of both positive and negative ions of single particles are then determined simultaneously in two time-of-flight reflectron mass spectrometers. The mass calibration for the time-of-flight signal was obtained by particles of known composition (i.e., elemental carbon containing particles give evident series of peaks, as described in section 3). Particles for which both size and mass spectra (positive and/or negative) are collected are classified as "hit." Particles which are sized but did not produce a mass spectrum are classified as "missed."

[9] The irradiance of the desorption/ionization laser (LDI) was kept at the maximum value, 109 W cm−2, because of the poor absorbing properties of the Mace Head aerosol. Alkali halide salts require a high laser fluence at 266 nm, depending on their light absorption and high lattice energy [Thomson et al., 1997]. Moreover, to be able to detect aqueous NaCl, the laser fluence has to be increased by more than four times compared to dry NaCl particles [Neubauer et al., 1997]. Mass spectra from non-sea-salt particles have also been observed to change dramatically with laser fluence [Noble and Prather, 1998; Silva and Prather, 2000].

[10] Recent studies have revealed that instrument sensitivities can be affected by both the size and the chemical composition of the particle being sampled. Allen et al. [2000] showed that particle detection efficiency conformed to a power law of diameter in the range 0.32–1.8 μm, decreasing by 2 orders of magnitude between 0.32

μm and 1.8 μm. Bhave et al. [2002], by comparing ion signal intensities from a single-particle mass spectrometer with quantitative measurements of atmospheric aerosol chemical compositions, showed that ATOFMS instrument sensitivities to nitrate and ammonium decline with increasing aerodynamic diameter over a range 0.32–1.8 μm. Recently, it has been reported that the most prevalent missed particle type during a filed campaign in Atlanta (Georgia, USA) was ammonium sulphate [Wenzel et al., 2003]. Although ATOFMS particle counts can be scaled to atmospherically representative concentrations by using a particle counter, in this study unscaled ATOFMS data are reported. During NAMBLEX, an aerodynamic particle sizer (APS) (Model 3320, TSI Inc. St. Paul, Minnesota, USA) and a Micro-Orifice Uniform Deposit Impactor (MOUDI) (MSP Corporation, Minneapolis, Minnesota, USA) were deployed concurrently with ATOFMS. A comparison between ATOFMS, APS, and MOUDI measurements can provide a better knowledge of the ATOFMS particle detection efficiency in a remote marine environment such as Mace Head, and a manuscript that describes these measurements is in preparation (M. Dall'Osto et al., ATOFMS scaling function: particle detection efficiency, chemical mass reconstruction and quantitative source assignment during NAMBLEX, 2004, hereinafter referred to as Dall'Osto et al., manuscript in preparation, 2004).

2.2. Data Analysis

[11] The commercial version of the ATOFMS (TSI 3800) uses two software packages, both of which are included with the instrument. The MassSpec operational software is a Windows®-based, C++ program that controls instrument operation. MassSpec also displays size, mass spectra, and time of detection for each individual particle in real time and saves all this information in a database (Microsoft® Access 2000 based). The MS-Analyze analytical software allows for analysis of the output from the MassSpec software. The positive and the negative spectra, together with the associated size of each particle, can be seen and various tables, graphs and average spectra can be calculated and displayed. All the information is stored in a Microsoft® Access 2000 data set, which can be queried (by using MS-Analyze or Microsoft® Access 2000) with specific searches. For example, the search can be based on particles of a specific size range or sampling period and presence, absence, or intensity of specific peaks.

[12] To qualify a mass/charge (m/z) ratio as a peak, a spectrum value had to be 20 units above a user-selected baseline, contain 20 square units of area and represent at least 0.005 as fraction of the total peak area of its spectrum. By choosing suitable ion markers in the individual particle mass spectra, the ATOFMS has the potential to describe changes in particle composition for a variety of chemical species in real time, including organic carbon, elemental carbon, metals, chloride, sulphate, nitrate, and ammonium.

2.3. Support Data

[13] Standard meteorological measurements were available as standard parameters at Mace Head. One-minute resolution data for wind speed, wind direction, relative humidity, and air temperature were recorded for the whole duration of the campaign. Additional information was derived from the use of calculated air mass back trajectories, allowing more detailed information on not only the local conditions

during the sampling but also on the history of the air masses during the previous several days.

[14] The back trajectories of air masses over a period of 5 days before arrival at Mace Head were available for 0000 and 1200 hours for each day of the whole campaign. A cluster of seven trajectories was calculated for each arrival time and detailed information regarding the methodology of calculation can be found elsewhere [Cape et al., 2000].

3. Results

[15] In all, 191,504 particles were recorded as "hits" during the NAMBLEX project, and their aerodynamic diameters and positive and negative spectra were recorded. The mean aerodynamic diameter of those particles was 1.46 ± 0.58 μm, while for of the missed particles (1,168,003) it was 1.2 ± 1.9 μm. Although similar, the size range of the particles hit by the ATOFMS is narrower than for those missed. The ablation process, along with the technical design of the ATOFMS, allows particles with an aerodynamic diameter between 0.3 and 3 μm to be hit.

[16] By performing searches based only on the presence or absence of various m/z signals belonging to different chemical species, the ATOFMS can provide a qualitative description of the aerosol composition. It is commonly cited that LDI analysis is a nonquantitative technique with enormous shot-to-shot variation [Gross et al., 2000], and it must be noted that in this study the data analysis refers to the numbers of particles containing the indicated chemical species and is not related to the mass of them. Additionally, inlet efficiency corrections, which are particle-size-dependent, have not been applied.

[17] The database was used to query the number of occurrences of a species of X Da in each hourly period. More than one m/z combination were used to classify a particle into different exclusive classes. The particles were then divided into general classes based on different queries to the database, giving three main broad chemical classes: (1) sea salt, (2) dust, and (3) carbon containing particles. The major classes were further qualified with all possible combinations of secondary species (sulphate, nitrate, and ammonium). Moreover, trace metals, e.g., vanadium and lead, were apportioned within different classes. As already explained in section 2, the power density of the desorption/ionization laser was kept at the maximum value, 109 W cm−2, which caused high fragmentation of the compounds in the particles detected [Silva and Prather, 2000]. As a result ion clusters with m/z higher than |120| were not often seen. A list of the relevant chemical markers used in this study is shown in Table 1. To ensure as far as possible that each particle could only belong to a single class (known as exclusive classification), functions AND and NOT were used.

Species	Tracer Ion	M/z (±0.5)	Peak Area	Function[a]	Particle Type Detected During the NAMBLEX, %
Pure sea salt	[Na]+	23	>40	AND	11.5
	[Na2Cl]+	81	>40	AND	
	[Cl]−	−35	>40	AND	
	[NO2]−	−46	>100	NOT	
	[Al]+	27	>100	NOT	
	[Fe]+/[CaO]+	56	>100	NOT	
Mixed sea salt	[Na]+	23	>40	AND	17
	[Na2Cl]+	81	>40	AND	
	[Cl]−	−35	>40	AND	
	[NO2]−	−46	>100	AND	
	[Al]+	27	>100	NOT	
	[Fe]+/[CaO]+	56	>100	NOT	
Aged sea salt	[Na]+	23	>40	AND	19
	[NO2]−	−46	>40	AND	
	[NO3]−	−62	>40	AND	
	[Al]+	27	>100	NOT	
	[Fe]+/[CaO]+	56	>100	NOT	
	[Na2Cl]+	81	>40	NOT	
	[C]+	12	>40	NOT	
Ca-rich particles	[Ca]+	40	>100	AND	3.5
	[CaO]+	56	>100	AND	
	[CaOH]+	57	>40	AND	
	[Na2Cl]+	81	>100	NOT	
	[Al]+	27	>100	NOT	
Al/Si-rich particles	[Al]+	27	>100	AND	2
	[SiO2]−	−60	>40	AND	
	[SiO3]−	−76	>40	AND	
	[Fe]+/[CaO]+	56	>100	NOT	
	[Na2Cl]+	81	>100	NOT	
Carbon-containing particles	[C]+	12	>40	AND	18
	[C3]+	36	>40	AND	
	[Al]+	27	>100	NOT	
	[Fe]+/[CaO]+	56	>100	NOT	
	[Na2Cl]+	81	>100	NOT	

Table 1. Summary of the ATOFMS Markers Used to Classify Species During the NAMBLEX Campaign at Mace Head, Ireland

[a]To belong at the particle type named pure sea salt, the "AND" function is a combination of the positive and the negative spectra of a particle detected by ATOFMS that must have a peak at m/z 23 ([Na]+) and a peak at m/z 81 ([Na2Cl]+) and a peak at m/z −35 ([Cl]−) and the "NOT" function does not peaks at m/z −46 ([NO2]−), m/z 27 ([Al]+), m/z 56 ([Fe]+, or [CaO]+).

[18] For example, the combination of the positive and the negative spectra of a particle detected by ATOFMS had to have a peak at m/z 23 ([Na]+) and a peak at m/z 81 ([Na2Cl]+) AND a peak at m/z −35 ([Cl]−) (referred to as the AND function) but not a peak at m/z −46 ([NO2]−) not a peak at m/z 27 ([Al]+) not a peak at m/z 56 ([Fe]+ or [CaO]+) (referred to as the NOT function) to belong at the particle type named pure sea salt. This "query and search" method is rigid and predetermined by the user, who decides the criteria after having looked at single mass spectra. An example of the limitation of not having any degree of flexibility in this classification can be found in single particle positive spectra with high peak areas at m/z 27 (aluminium) and at m/z 56 (calcium/iron). The two dust particle types listed in Table 1 are named "Ca-rich" and "Al/Si-rich" particles, and they exclude the presence of one of the two peaks indicated above, depending the type considered. A single particle positive spectrum with a strong signature (peak area >100) both at m/z 27 (aluminium) and m/z 56 (calcium/iron) would result in the unclassified particles type. By considering peaks with peak area higher than 100 (absolute intensity as reported by the instrument) either for m/z 27 and m/z 56, the limitation of this classification was reduced, i.e., a particle with a strong m/z 27 signal (>100), along with its combination of peaks listed in Table 1, and a weak m/z 56 signal (<100) was still classified as "Al/Si particles." However, the ATOFMS data set collected during NAMBLEX was not strongly affected by this problem because mass spectra were generally unique, and the combinations of different peaks (e.g., strong signature of both aluminium and calcium/iron) were not often observed. It must be noted the classification shown in Table 1 (created after a detailed visualization of the single-particle mass spectra) works for this specific data set, and it is likely it would not work for a more complex data set such as one created in a more polluted environment, where either the positive and the negative mass spectra of the particle sampled present many more peaks. The alternative to this type of rigid defined classification is to use advanced supervised and unsupervised statistical methods [Song et al., 1999; Pastor et al., 2003], and one element of work in our laboratory is directed at applying such methods to our ATOFMS data and will be reported at a later date.

[19] The size, the time of detection, and the positive and the negative m/z peak ratios of each of the 191,504 particles were placed in a Microsoft Access 2000 database from which it was possible to query the number of occurrences of each combination of markers used to describe a class in each hourly period. The queries were always applied to the full database, and not after withdrawal of particles of other types. Table 1 shows the relative abundances of the various particle types. In all, some 71% of particles were classified. Overlap between the categories is minimal. The largest overlap was between the aged sea salt and carbon classes, with 1850 (<1%) particles meeting the criteria for both categories.

[20] The failure to classify a particle generally originated for one of two main reasons. The former is as explained above because of the rigidity of the classification used. The latter, more important reason, originated from the low signal/noise ratios in some single mass spectra. Most of the unclassified particles presented only two distinguishable m/z signals (m/z 23 [Na]+ and m/z 39 [K]+) in the positive spectrum and none in the negative. These particles are therefore unlikely to contain significant different classes of particles. The ATOFMS is very sensitive to alkali metal cations [Gross et al., 2000], and since sodium and potassium are present in large abundance in

sea-salt particles, it is not surprising that these are the only peaks visible in some spectra.

3.1. Sea Salt

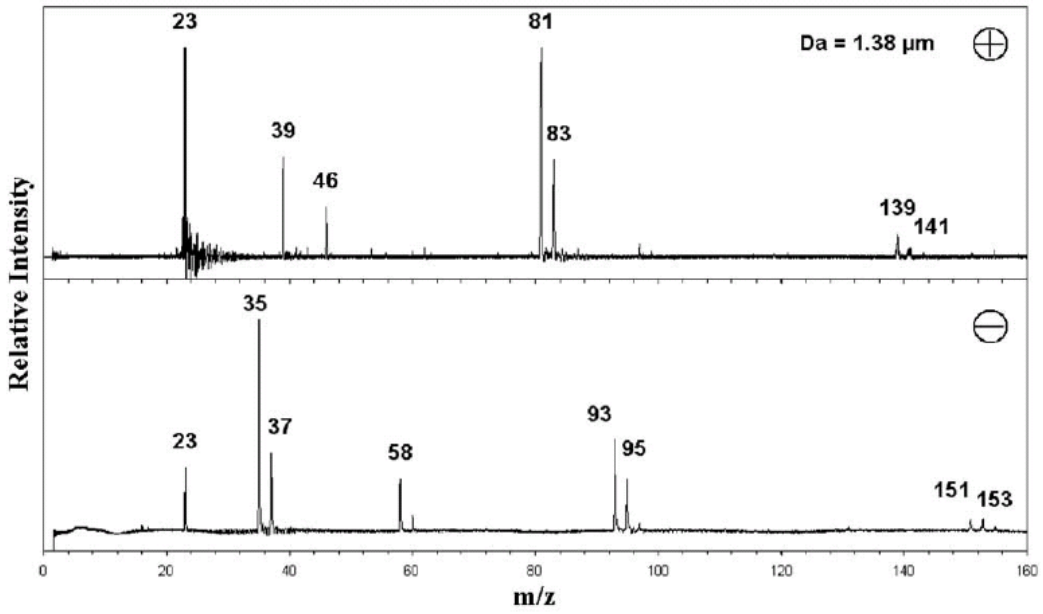

Figure 1. Typical aerosol time-of-flight mass spectrometer (ATOFMS) single-particle positive (plus) and negative (minus) mass spectra of a particle attributed to the pure sea-salt category.

[21] The global emission of sea-salt particles is more than 20 times the combined emissions of organics, black carbon, sulphate, nitrate, and ammonium into the atmosphere [Raes et al., 2000]. Aerosol at Mace Head has a strong marine source [Arimoto et al., 1995; Huang et al., 2001]. An example of the most common laser desorption/ionization mass spectra from an individual pure sea-salt particle detected during the campaign is shown in Figure 1. Almost all of the peaks observed are attributable to sodium chloride clusters. In the positive ion spectra, peaks are present for [Na]+ (m/z 23), [K]+ (m/z 39), [Na2]+ (m/z 46), [Na2Cl]+ (m/z 81 and 83), and [Na3Cl2]+ (m/z 139 and 141). In the negative spectra, peaks are present for [Na]− (m/z 23), [Cl]− (m/z 35 and 37), [NaCl]− (m/z 58 and 60), [NaCl2]− (m/z 93, 95 and 97), and [Na2Cl3]− (m/z 151, 153 and 155). Several other peaks due to other compounds, i.e., [K2Cl]+ (m/z +113), [KCl2]− (m/z −109), and [NaKCl]+(m/z +97), were observed occasionally during the campaign. Liu et al. [2003] reported a unique type of sodium particle mass spectra where sodium was detected with water cluster ion signals. We also observed the presence of peaks at 41, [Na(H2O)]+ and 59, [Na(H2O)2]+ in several mass spectra at Mace Head. Moreover, some unique types of negative sodium chloride clusters were observed during NAMBLEX. Peaks at m/z −111 and −129 were attributed to [NaCl2(H2O)]− and [NaCl2(H2O)2]−, respectively. The presence of water in pure sea-salt particles was confirmed by the presence of peaks at m/z −16 [O]−, −17 [OH]−, −46 [Na2]−, 62 [Na2O]+, and 63 [Na2OH]+. It is important to note that these peaks were detected in pure sea-salt particles only when the relative humidity was higher that 90%. Sodium chloride has a deliquescence relative humidity (DRH) (the equilibrium RH at which solid particles become aqueous

droplets) of 75% [Neubauer et al., 1998] but during all the episodes of pure sea-salt particles detected the RH was never lower than 75% so we cannot present any spectra of dry particles of sodium chloride. The sodium chloride cluster at m/z 81 [Na2Cl]+ was the most common in the positive spectra, while most common in the negative spectra was the peak at m/z −93, [NaCl2]−. Therefore our results are consistent with studies on alkali metal halides which have reported singly charged clusters, especially cation excess clusters of the type [(CA)nC]+, where C and A represent the cation and anion of the molecule [Zhang and Cooks, 2000]. In contrast, Neubauer et al. [1998], using similar desorption-ionization wavelength (248 nm), did not report the presence of these peaks at relative humidities above 70%, although in their study a lower desorption-ionization laser fluence (1.7 J cm−2), in comparison with the one used in ours (5 J cm−2), was employed.

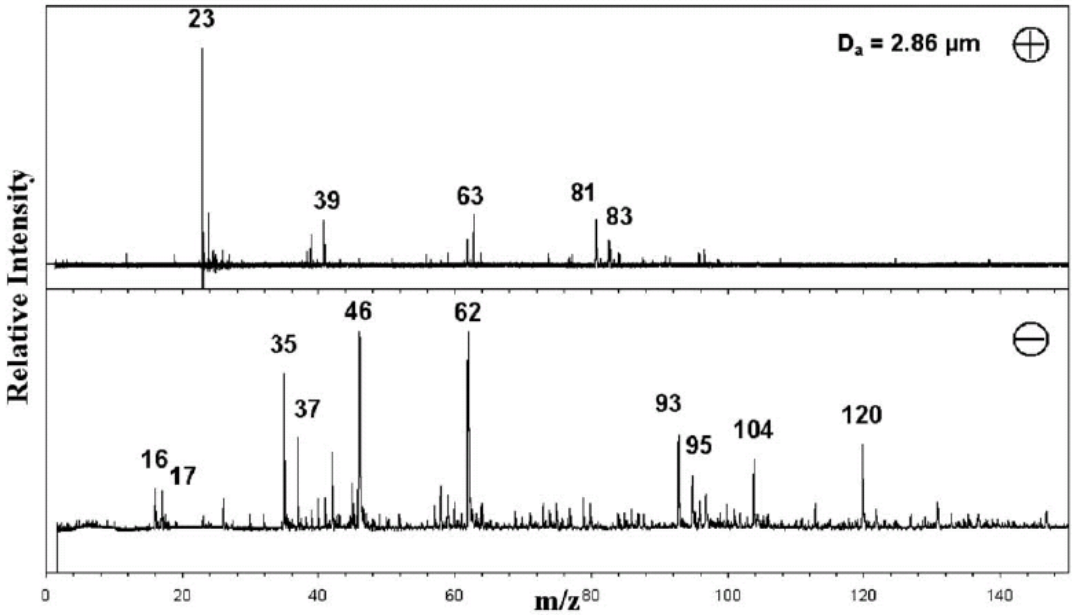

Figure 2. Typical ATOFMS single-particle positive (plus) and negative (minus) mass spectra of a particle attributed to the mixed sea-salt category.

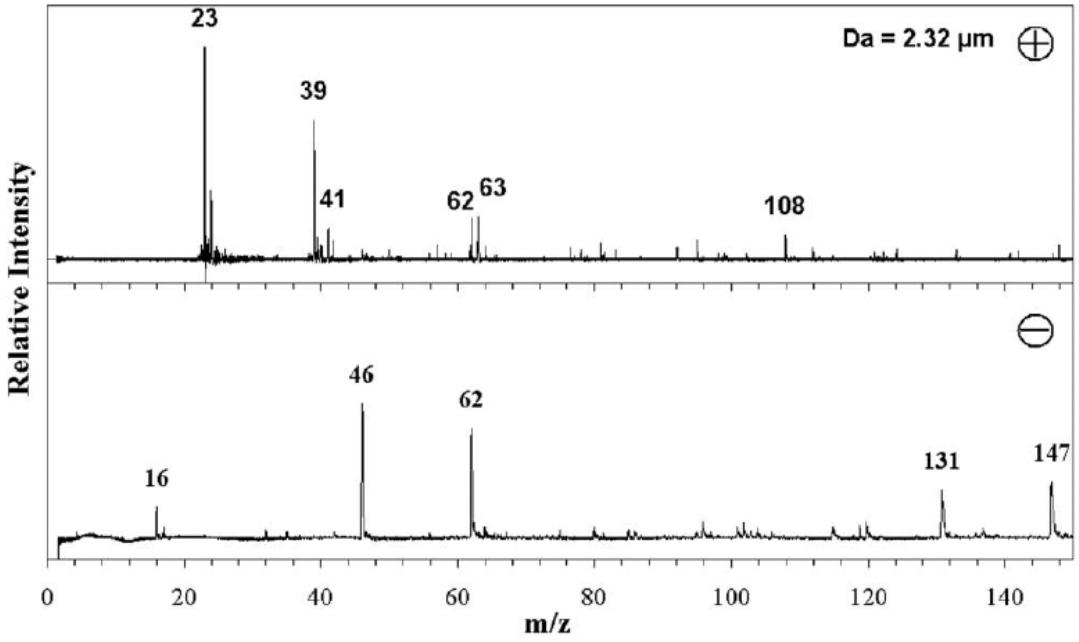

Figure 3. Typical ATOFMS single particle positive (plus) and negative (minus) mass spectra of a particle attributed to the aged sea-salt category.

[22] Sea-salt aerosols can react with HNO3 to form nitrate and release hydrogen chloride to the gas phase [Harrison et al., 1994; Harrison and Pio, 1983; Pakkanen, 1996]. These aging processes change the physicochemical properties of sea-salt aerosols. In Figure 2, mass spectra are displayed in which, in addition to the usual sodium chloride clusters peaks, peaks indicating the presence of nitrate, at mass-to-charge 63 [HNO3]+, −46 [NO2]−, −62 [NO3]−, −104 [(NaCl)NO2]−, and −120, [(NaCl)NO3]− are seen. In Figure 3 another spectral type is shown in which all the peaks corresponding to NaxClyNOz clusters are replaced with NaxNOy clusters. The peaks at 108, −131, and −147 indicate the presence of [Na2NO3]+, [NaNO2NO3]−, and [Na(NO)2]−, respectively. In addition to nitrate, sea-salt particles can also uptake sulphate by condensation of sulphuric acid from the gas phase and by converting dissolved SO2 to sulphate. However, according to other analysis [Kerminen et al., 1998], condensation of gaseous sulphuric acid to sea-salt particles usually has negligible influence in comparison to nitric acid. In our study only 5.8% of aged sea-salt particles were internally mixed with sulphate, and therefore only the reaction of sea-salt particles with gaseous nitric acid will be discussed further in this section. A selection of characteristic m/z combinations were used to apportion into three different subclasses of sea-salt particles: pure, mixed, and aged sea salt. Although the ion [Na2NO3]+ (m/z 108) has previously been used to indicate the heterogeneous replacement of chloride by nitrate in individual sea-salt particles [Gard et al., 1998; Song et al., 1999], in this study several different combination of peaks were investigated. The reason was due to the higher frequency of peaks of smaller m/z detected during the campaign, i.e., m/z 63 [HNO3]+/[Na2OH]+, −46 [NO2]−, and −62 [NO3]−. In all the sea-salt type mass spectra with a signal at m/z 63 and/or at m/z −62, a peak at m/z −46 was also present. The peak at m/z 63 can be attributed either to [HNO3]+ or [Na2OH]+, although the latter is more likely, because of its lower ionization potential.

[23] Several mass spectra showed peaks at m/z 23, 81, −35, and −46 but not at −62 or 63. A higher value of area (100) for m/z −46 than for other peaks was chosen to avoid interference with the weaker signal of [Na2]−. The combination of markers for describing unreacted, mixed, and aged sea salt are provided in Table 1, and in Figure 4a the temporal trends of the three subclasses are presented. It can be seen that between 1 and 6 August 2002, when eastern air masses were arriving at Mace Head, the major proportion of sea salt is aged. Air masses trajectories also confirm that particles exchanged a significant fraction of chloride during air mass stagnation over the ocean. In fact, the bursts of mixed and aged sea salt are associated with periods of very slow moving air. As expected, the maximum pure sea-salt contribution was when air masses were coming straight from the clean sector (180°–250°). This is consistent with another study [Kleefeld et al., 2002] at Mace Head in which the sea-salt concentration showed an increase with increasing local wind speed (6–12 m s−1), reflecting the production of sea-salt aerosols within the surf zone.

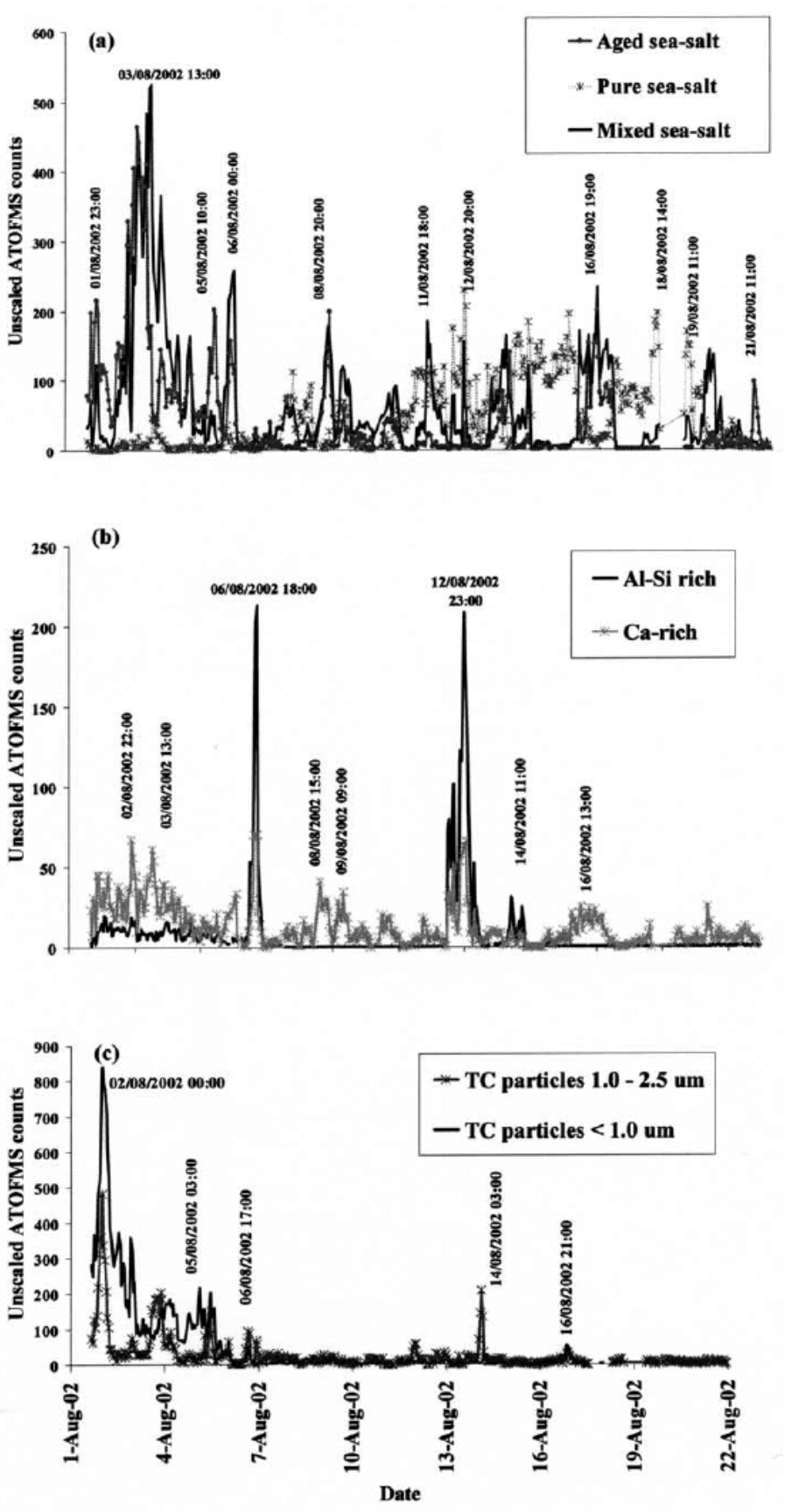

Figure 4. Hourly average temporal trends of (a) pure, mixed, and aged sea-salt particles; (b) dust particles, Ca-rich and Al/Si-rich types; and (c) carbon particles.

3.2. Dust

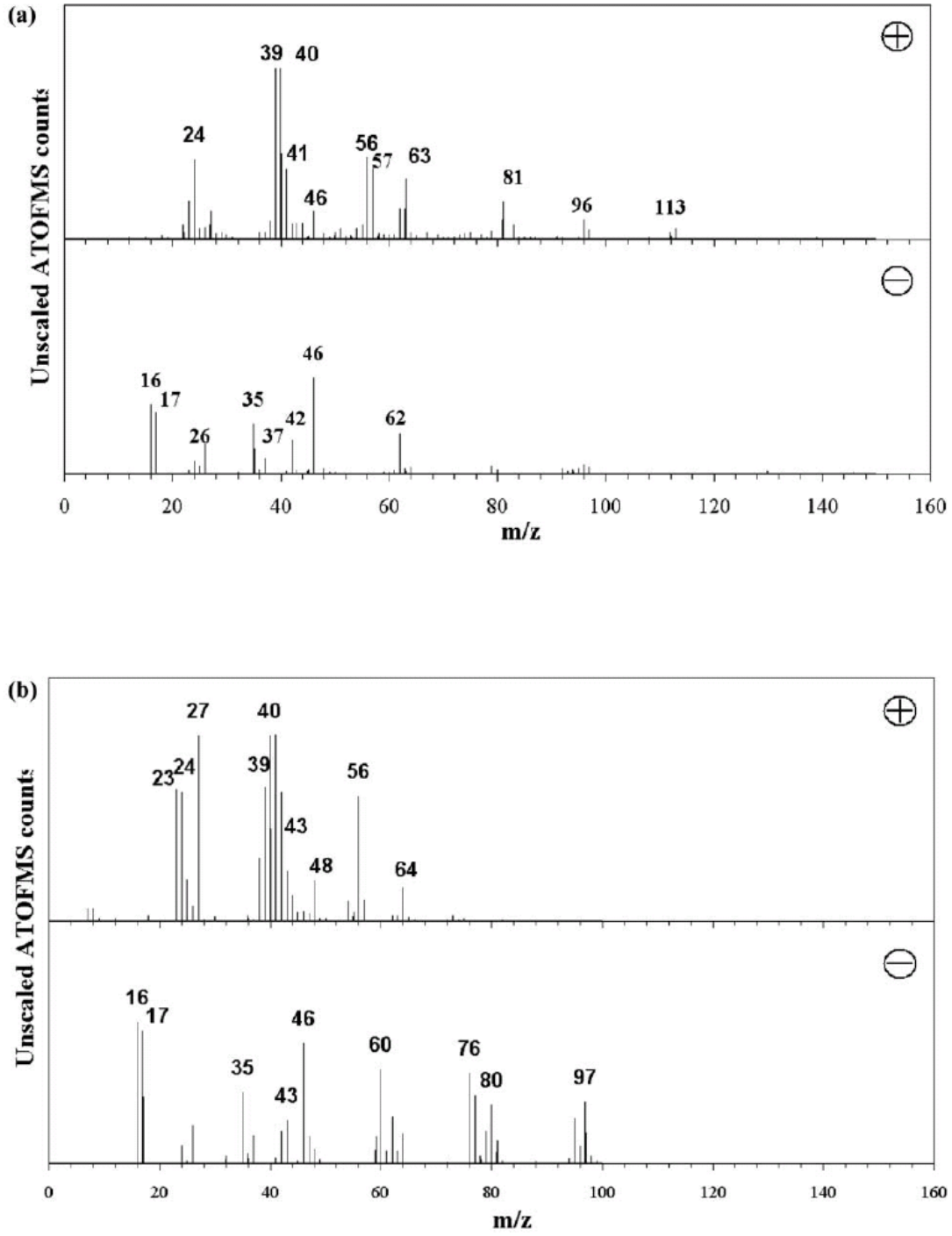

Figure 5. Average positive and negative spectra for (a) Ca-rich particles and (b) Al/Si-rich particles (Saharan dust).

[24] Another significant contributor to global tropospheric particulate matter is suspension of soil dusts or other crustal material. This is considered the second largest global primary source after sea salt [Raes et al., 2000]. The most common species used for searching for crustal materials were aluminium (m/z 27), calcium (m/z 40 and 56), titanium (m/z 48 and 64), lithium (m/z 7), iron (54 and 56), and silicate (−60

and −76). Owing to the presence of [CaO]+ at m/z 56 which interfered with Fe+ (m/z 56) and the lack of iron clusters detected, a combination of m/z 54 and 56 was chosen to identify iron, which corresponds to the two most common isotopes (54Fe and 56Fe). The presence of two peaks for describing titanium and silicate was also necessary to avoid interference with elemental carbon ([C4]+ and [C6]−). Two distinct classes of dust particles were identified: Ca-rich particles and Al/SiOx− rich particles. Figures 5a and 5b show the positive and the negative ion spectra of the two kinds of particles. Both types show peaks for sodium (m/z 23), magnesium (m/z 24, 25), potassium (m/z 39), chloride (m/z −35, −37), and oxygen (m/z −16, −17). In addition, peaks for calcium (m/z 40 [Ca]+, 56 [CaO]+, 57 [CaOH]+, 96 [Ca2O]+ and 113 [Ca2O2H]+), and nitrate (m/z −46, −62) are present for Ca-rich particles. In the Al/Si-rich particles, peaks of silicate at m/z −60 [SiO2]− and −76 [SiO3]− dominate the negative spectra. In the positive spectra, peaks at m/z 48 and 64 are attributed to titanium as [Ti+] and [TiO]+. The chemical heterogeneity observed in dust particles is the result of various chemical species, as shown in Table 2. It can be seen that nitrate peaks occur much more frequently in Ca-rich particles (65%) compared to Al/Si-rich particles (45%). Atmospheric coarse particle NO3− is formed in the reaction of nitric acid with Ca-rich soil dust [Pakkanen, 1996; Yeatman et al., 2001].

Dust Type	Chloride, %	Nitrate, %	Sulphate, %	Ammonium, %	Titanium, %	Phosphate, %	Carbon, %
Al/Si rich	65	45	40	9	52	17	2
Ca rich	65	65	10	7	12	15	2

Table 2. Frequencies of Different Species in Ca-Rich and Al/Si-Rich Particles

[25] Zhuang et al. [1999] report that HNO3, SO2, or H2SO4 can react with aqueous carbonates such as dissolved CaCO3 and MgCO3 on soil particles to form coarse mode nitrate and sulphate. Non-sea-salt sulphate formed by the reaction of H2SO4 with soil compounds has also been reported [Pakkanen, 1996; Yeatman et al., 2001]. However, it is not possible to differentiate between those species in soil particles which are due to the original chemical composition of the particles and those arising from reactions with compounds such as nitric or sulphuric acid.

[26] Both types of particles showed a low frequency of carbonaceous peaks (<2%). Phosphate (m/z −63 [PO2]− and m/z −79 [PO3]−) was present at a similar percentage, 17% (Ca rich) and 15% (Al/Si rich) in both classes. The temporal profile of this ion, as well as fluorine (m/z −19), tracked that of dust particles, suggesting their major source is dust particles. Phosphates have often been associated with soil dust, their frequency of occurrence varying between 10 and 30% [Silva et al., 2000; Silva et al., 1999].

[27] Lithium was found in 31% of particles classified as dust particles. It is important to note that this cation was found only in these classes. Barium was not found in either type of dust particle. Titanium was strongly associated with Al/Si-rich particles ($R2 > 0.9$), indicating the possibility to use it as a marker of this class. Chloride was present in about 65% of particles classified as dust particles. The main occurrence of chloride at Mace Head is obviously from sea-salt particles, although

soil particles represent another source. Soil and sea-salt particles provide the main contribution to the chloride-containing population. The 74.5% of chloride-containing particles were due to sea salt apportioned as mixed sea salt (58%) and pure sea salt (42%). Al/Si-rich and Ca-rich particles contribute 5 and 7%, respectively, to the number of chloride-containing particles. Chloride was mainly distributed in the coarse (>1 μm) mode, and only one short episode of fine chloride particles was recorded on 5 August between 0100 and 0200. On further analysis of these mass spectra, association with carbon, potassium and lead was also found. These particles were the only lead containing particles detected during the campaign and they might have been generated from a combustion source near the site. In Figure 4b the temporal trends for the two types of dust particles, Ca-rich and Al/Si-rich particles, are reported.

[28] Arimoto et al. [1995] compared the Mace Head site with the Barbados, Bermuda, and Izana sites and showed that Mace Head has the lowest dust concentrations but the highest sea-salt concentrations. One of the reasons is that Mace Head tends to have more marine influences because of its high latitude. However, Huang et al. [2001] reports two crustal classes, which have two different sources, one Ca-poor likely to come from the Sahara and one Ca-enriched from Mace Head local rock and soil. While local soil sources are Ca-enriched, Saharan dust is depleted relative to most crustal material. As seen in Figure 4b, the Ca-rich type occurs more frequently, suggesting a local origin. It is well established that Saharan dusts are dominated by SiO2 and Al2O3 [Goudie and Middleton, 2001].

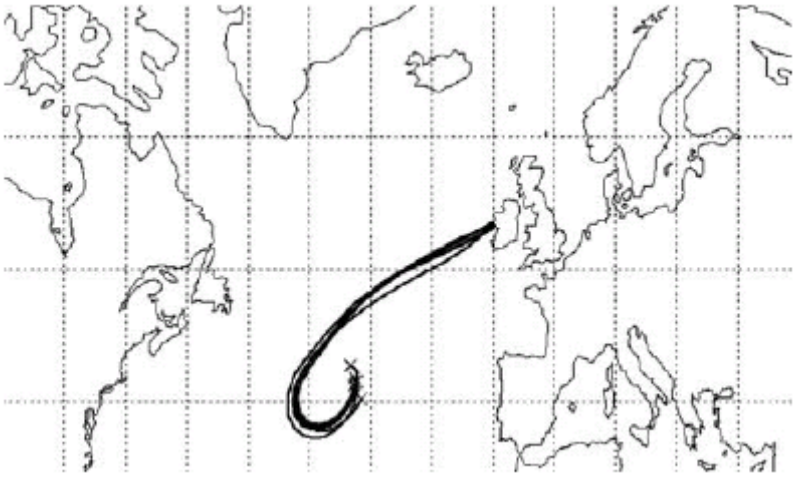

Figure 6. Five-day back trajectories arriving at Mace Head (Ireland) at 1200 LT on 8 December 2002.

[29] A number of studies have focused on the long-range transport of Saharan air masses over western and eastern North Atlantic areas [Bergametti et al., 1989; Morales, 1986; Rajkumar and Chang, 2000] and across the Mediterranean [Chester et al., 1984; Rodriguez et al., 2001] into central Europe [Monn et al., 1995]. Long-range transport of Saharan dust across the British Isles appears to be much less frequent than for southern and central Europe and both North and South America [Ryall et al., 2002]. As shown in Figure 4b, Al/Si-rich type dust particles show a very temporally variable occurrence. They have a small continuous presence in the first part of the campaign, between 1 and 5 August, when dirty air masses were coming from the east, and as three sharp episodes at 1600 on 6 August 2002, 2300 on 12 August 2002 and

1100 on 14 August 2002. The low continuous presence of the first part of the campaign was not apportioned and is probably due to different European sources. In contrast, the air mass back trajectories revealed that during the three sharp episodes air was coming from the southwest, as shown in Figure 6 for 8 December 2003. Five-day back trajectories for 1200 on 6, 13, and 14 August 2002 were very similar.

[30] It is important to note that these three episodes were the only ones where air was coming from the direction reported. These episodes of the Al/Si-rich particle type also showed a strong correlation with relative humidity and local wind direction. Wind speed was highly variable and fluctuated between 5 and 10 m s−1, while RH was always higher than 97% and the wind direction always 230 ± 2°. It appears that this particle type arises only when specific air masses from the SW arrive at Mace Head, suggesting long-range sources of this class of dust particles. Despite the nominal clean sector lying between 180° and 300°, we believe that the particles arise from long-range transport of Saharan particles since the 5-day back trajectories indicate an origin from the Azores high-pressure region which can draw air from North Africa.

[31] Previous studies [Ryall et al., 2002] have examined the frequency of long-range transport from the Sahara region to the British Isles over a 5-year period, analyzed by means of a sophisticated Lagrangian dispersion model. Although considerable literature is available on the mineral and chemical composition of Saharan dust, transport patterns of selected dust outbreak events, and the influence on deposition chemistry, there is limited information on the impact of Saharan dust on the measurements of air quality monitoring networks. Analyses of PM10 measurements at Lough Navar, a rural monitoring site in Northern Ireland (UK) some 180 km to the northeast of Mace Head, show a number of significant episodes between 1995 and 2000 resulting in elevated PM10 concentrations because of transport of air from the Sahara. We have analyzed hourly PM10 data from Lough Navar for August 2002. The hourly PM10 concentrations during the episodes in which we detected Al/Si dust particles were lower than 10 μg m−3 for the entire campaign, suggesting the occurrence of Saharan dust episodes might be much more frequent than has been concluded previously on the basis of excursions in PM10 mass concentrations.

3.3. Carbon

[32] Carbonaceous aerosol is a complex mixture of substances, usually classified into two main fractions, black carbon (BC) and organic carbon (OC). Black carbon is also known as elemental carbon (EC) [Castro et al., 1999].

[33] While black carbon is essentially a primary pollutant, emitted directly during the incomplete combustion of fossil and contemporary biomass carbonaceous fuels, organic carbon has both a primary and secondary origin. Submicron primary particulate organic carbon (<1 μm) is emitted directly during combustion processes, while the supermicron mode (>1 μm) is produced mainly by mechanical processes, associated with the emission of plant spores and pollen, vegetation debris, tire rubber, and soil organic matter. Particulate organic carbon has also a secondary origin from gas to particle conversion of volatile organic compounds in the atmosphere. Castro et al. [1999] reported, as expected, a very low carbonaceous matter concentration at Mace Head compared with urban areas. In their study, a high value of 10.8 for the

ratio OC/BC suggests that in the summer there is increased formation of secondary organic carbon, because of more favorable conditions for gas/particle conversion. Kleefeld et al. [2002] report the mass concentrations of total organic carbon (TOC) and its chemical fractions, water-soluble organic carbon (WSOC), water-insoluble organic carbon (WISOC), and black carbon (BC) measured at Mace Head. WSOC was found to be the dominating fraction in "modified marine aerosol samples," followed by WISOC and BC, whereas in "clean marine aerosol samples" WISOC was the main fraction, followed by WSOC and BC.

[34] Particles containing carbon (defined as TC) were determined in marine aerosols sampled during the campaign. An attempt was made to attribute TC to biogenic or anthropogenic sources, according to the chemical composition and the origin of air masses arriving at Mace Head. Particles containing elemental or organic carbon yielded characteristic signatures in the positive and negative mass spectra with progressions of Cni and CnHmi ions, respectively [Liu, 2003; Wenzel, 2003]. Values of n and m were typically 1–10 and 1–3, respectively. Peaks at m/z 27 and 43 were often seen, which correspond to [C2H3+] and [(CH3)CO]+, respectively. After having investigated several different criteria, particles with a mass spectrum having peaks at m/z 12 and 36 were classified as carbon containing particles. This is based on the following reasoning: Peaks with m/z ratio higher that 72 were not often seen; moreover, [Mg]+ interferes with [C2]+ (m/z 24), [Al]+ interferes with [C2H3]+ (m/z 27), [Ti]+ interferes with [C4]+ (m/z 48), and [SiO2]− interferes with [C5]− (m/z −60). Figure 4c shows the temporal variation of particles containing carbon, defined using m/z 12 and 36. It is clear that the campaign can be split into two periods: The former, between 1 and 6 August 2002, with high concentrations of carbon containing particles, occurred when Mace Head was subjected to a dirty continental air mass from Europe, and the latter, between 6 and 21 August, was associated with generally clean air masses. Three other minor episodes were noted during the campaign, on 11, 14, and 16 August 2002. These episodes were correlated with aged sea-salt aerosol bursts, when dirty air was arriving at Mace Head. Back trajectories revealed air masses arriving at Mace Head from the west, suggesting polluted air masses from North America. It is important to note that dirty air masses coming from USA/Canada bring carbon-containing particles associated with sodium that are distributed predominantly in the coarse mode, suggesting secondary formation on existing particles. During the whole campaign 17.7% of particles were classified as carbon-containing particles, 85% of these were detected during the first 6 days, and 67% of carbon-containing particles had an aerodynamic diameter smaller than 1 μm. They were internally mixed in different percentages with other ions: 15% with ammonium, 11% with nitrate, and 36% with sulphate. The degree of mixing of different species was calculated as the presence of characteristic peaks in the positive and in the negative spectra. The whole ATOFMS data set was queried, and the percentages represent the abundance of different species in the whole data set. They do not represent the entire atmospheric particle population sampled during NAMBLEX, although the large number of particles sampled allows some inferences to be drawn.

[35] On inspection of single mass spectra of TC particles, it is important to note that the degree of mixing with secondary species changed remarkably with particle size. The average mass spectra of particles in the ranges 0.2–0.5 μm, 0.5–0.7 μm, and 0.7–1 μm did not exhibit any major difference. Peaks representing carbon (m/z 12, 24, 36, 37, and 48), potassium (m/z 39), and sulphate (m/z −97) dominated the positive and

negative average spectra. However, in particles >1 μm, peaks at m/z 23, −46, and −62 are also present. They can be attributed to sodium (m/z 23) and nitrate (m/z −46, −62). The presence of sulphate in coarse particles (>1 μm) was clearly indicated by the peak at m/z −80 [SO3]−.

[36] TC particles were more often mixed with nitrate in the coarse mode rather than the fine mode, 29 and 3% respectively. The degree of mixing with sodium in TC particles shows the same trend, with 90% of coarse TC particles associated with it, while only 7% of the fine mode. Inorganic carbon in aerosols exists mainly in the form of carbonate, and the most likely carbonate minerals are calcite (CaCO3) and dolomite [CaMg(CO3)2]. However, Kleefeld et al. [2002] reported that inorganic carbon could be neglected in the TC content of aerosol at Mace Head and concluded that the enhanced concentrations of water insoluble organic carbon (WISOC) during summertime in clean marine aerosol samples could be due to primary biological particles, derived for example from marine microorganisms. This explanation was supported by a general correlation between WISOC and sodium, which is injected into the atmosphere in jet drops together with marine organic matter. An attempt to select carbon-containing particles associated with sodium (m/z 12 [C]+, 36 [C3]+, and 23 [Na]+) was insufficiently specific because most aged sea-salt aerosols were distributed in the coarse mode. A specific feature of the aged sea-salt aerosols is their enrichment with organic matter [Castro et al., 1999; Cooke et al., 1997; Jennings et al., 1993] which it is not possible to distinguish from biogenic aerosol. Selenium and iodine, which are usually markers for biogenic emissions [Huang et al., 2001] were not detected with the ATOFMS.

[37] EC is often used as a tracer for anthropogenic combustion of fossil fuel in the Northern Hemisphere and the source strength is expected to be relatively constant throughout the year [Cooke et al., 1997; Jennings et al., 1993]. The monthly average elemental carbon concentration between 1989 and 1996 at Mace Head was quite low, 50 ng m−3 [Cooke et al., 1997]. The average EC concentrations were >100 ng m−3 when easterly winds occurred over protracted time periods and transported continental air masses as far as Mace Head. Identification of elemental carbon with the aerosol time-of-flight mass spectrometer was attempted. The criterion used to search for elemental carbon was the presence of high carbon cluster ions, [Cn]+. Peaks at m/z 60, 72, and −72, [C5]+, [C6]+, and [C6]− respectively, had to be present to classify a particle as elemental carbon type. Using this criterion, 0.33% of particles detected were classified as elemental carbon (EC), representing 1.9% of TC particles. The percentage is lower than reported by Kleefeld et al. [2002], who found the percentage contribution of EC to TC mass to be 21 ± 2%. It is important to note that the high laser fluence (109 W cm−2) of the LDI laser used during our campaign gave a considerable fragmentation of organic compounds. It has been observed, for example, that at high laser fluence (109 W cm−2) considerable fragmentation of PAH occurred, whereas a low laser fluence (108 W cm−2) produced the parent ion (M+) with very little fragmentation [Silva et al., 2000]. Moreover, owing to the different possible fragmentations during the LDI process itself, we were unable to provide a rational apportionment between TC and EC. When analyzing single particle mass spectra, particles containing internally mixed elemental carbon (EC) and organic carbon (OC) were detected. In addition to peaks of elemental carbon cluster [Cn]±, organic fragments with peaks at m/z 27 [C2H3]+ and m/z 43 [CH3CO]+ as well as presence of [CnHm]± hydrocarbon clusters were recorded. It is important to note that all the

particles classified as containing EC were detected only during episodes of dirty air, coming either from America or Europe.

[38] Sodium and potassium were the two elements most commonly associated with carbon. Another element found to be associated with carbon was vanadium. Even though vanadium is widely distributed throughout the lithosphere, it is not present in high concentrations in minerals. V originates from primary sources such as ores, metallurgical slags, and petroleum residues [Moskalyk and Alfantazi, 2003]. As well as V being present in specific types of iron ores and phosphate rock [Poledniok and Buhl, 2003], the element is detected in some crude oils in the form of organic complexes [Vitolo et al., 2000]. Several dust and rock samples were collected near the site at Mace Head and analyzed in the laboratory with ATOFMS; none of them showed the presence of vanadium. The criteria used for searching V-containing particles was a combination of peaks at m/z 51 and 67, corresponding to [V]+ and [VO]+, respectively. Of the total particles chemically analyzed during the NAMBLEX campaign 1.1% contained vanadium, and 75% of them were detected during the first 4 days of the campaign, when polluted air was arriving from Europe. Vanadium-containing particle mass spectra detected during that period were highly associated with carbon (70%), iron (60%), sulphate (55%), and nitrate (30%). Vanadium- containing particles were detected also during pollution episodes associated with air masses originating from the northeastern United States. Such vanadium-containing particles were internally mixed with various species. While organic marker ions typically accompanied vanadium-containing particles in European originated air masses, there was no evidence of carbon peaks in vanadium-containing particles generated in the northeastern United States. The mass spectra of these particles typically contained signals from magnesium, iron, chloride, nitrate and sulphate, indicating different sources of vanadium. It is likely that vanadium-containing particles from Europe have a crude oil origin, whereas the wholly inorganic signature of vanadium-containing particles coming from North America suggests a metallurgic pollution origin.

3.4. Secondary Species

[39] Particulate matter can be broadly separated into primary and secondary. Secondary particles are those formed through chemical transformation of gas-phase species in the atmosphere, most notably sulphur dioxide, oxides of nitrogen, and volatile organic compounds [Harrison et al., 1999]. Although associations between primary and secondary particles have been reported in the previous sections, this section examines them more systematically. The extent of secondary species in the three broad particle types that were classified is examined, and it is shown how secondary species can be differentially internally mixed in the classes apportioned and in different size modes.

[40] Only particles with both positive and negative ion spectra are included in the analysis. The negative spectra were vital for identifying sulphate (m/z −97, [HSO4]−) and nitrate (m/z −46 [NO2]− and m/z −62 [NO3]−), while the positive spectra were used for ammonium (m/z 18 [NH4]+) and carbon (m/z 12 [C]+ and 36 [C3]+). Associations between carbon-containing particles and secondary species have already been described and so will not be discussed in this section.

[41] Aerosol nitrate is predominantly anthropogenic and arises from the oxidation of NOx (NO and NO2) which is produced mainly in the high-temperature combustion processes associated with vehicles and industrial activity [Harrison et al., 1999]. Nitrate-type particles have already been described in the previous subsections, so only a summary is given here. Liu et al. [2000] employed a peak in the positive spectrum at m/z 30 [NO]+ to track nitrate containing particles. In our study, this peak was not observed. It seems likely from past campaigns conducted in Birmingham (UK) that the peak at m/z 30 occurs only with urban aerosols, where the concentrations of carbon and nitrate in the particles are much higher. Some 28% of particles detected during the campaign were nitrate-containing types, of which 93% were sea-salt types: 54% mixed sea-salt particles and 39% aged sea-salt particles, respectively. The other minor occurrence of nitrate aerosol was due to soil dusts (5%). On inspection of size-composition relationships, only 6% of nitrate was in the fine mode and this was typically coupled with potassium and sulphate.

[42] Non-sea-salt sulphate (nss-SO42−) is a mixed source tracer with a large anthropogenic fossil and biomass fuel component and a smaller biogenic marine component. The interpretation of its presence is further complicated by the chemical reactions of SO2 on dust particles. Savoie et al. [2002] estimate that the biogenic source accounts for about 10–15% of the total annual average nss-SO42− at Mace Head. Common ATOFMS signals attributed to sulphur species occur at m/z −64 [SO2]−, −80 [SO3]−, −96 [SO4]−, and −97 [HSO4]−. Particular attention was given to m/z −96 and −97 which can interfere, with weak signals due to chlorine isotopes in [NaCl2]− such as [Na37Cl37Cl]− (m/z −97). To overcome this problem an absolute area of at least 100 at m/z −96 and −97 was required as a criterion for the presence of sulphate rather than a minor interfering peak.

[43] We confirm the studies of Liu et al. [2003] that found these peaks to be more often coupled with dust and organic particles, whereas the best marker of sulphate in sea-salt particles was the peak at m/z 165 [Na3SO4]+. As already shown in Figure 1, sea-salt sulphate was not detected in pure sea-salt particles. However, the presence of a peak at m/z 165 [Na3SO4]+ was vital for indicating nss-SO42− in sea-salt particles.

[44] Fourteen percent of particle mass spectra obtained with the ATOFMS between 1 and 21 August 2002 at Mace Head contained a signal at m/z −97, which was the primary marker for sulphate; 46% of these were internally mixed with carbon. Further analysis of particles binned in different size ranges showed that sulphates in the submicron mode (<1 μm) are more usually coupled with carbon (68%) than those in the supermicron mode (35%).

[45] In general, sulphate-containing particles were associated with carbon and potassium in both the fine and coarse mode but with sodium only in the coarse mode. Sulphate particles were therefore apportioned into fine (15%) and coarse (85%) particles, suggesting different sources. While the former probably originated from combustion processes, the latter represent the product of heterogeneous reactions of SO2 with dust and the physical or chemical adsorption of gaseous species on aerosol particle surfaces.

[46] Sea salt particles, in general, did not show a peak attributable to sulphate in the negative spectra. A second ATOFMS marker, [Na3SO4]+ (m/z 165), was used to

indicate non-sea-salt sulphate in sea-salt particles. Particle mass spectra with a peak at m/z 165 also contained peaks due to sodium, potassium, chloride and nitrate. This type of particle was frequently internally mixed with nitrate (90%) and was detected only during episodes when polluted air masses were advected from mainland Europe and North America. Although the reaction between H2SO4 and NaCl is limited by the typically low concentration of gas-phase H2SO4 [Kerminen et al., 1998; Roth and Okada, 1998], both nitrate and sulphate are developed in sea-salt particles because of uptake of NOx, HNO3, and SOx. However, it should be noted that sulphate is not well detected by the ATOFMS.

[47] A laboratory-based study [Thomson et al., 1997] has indeed demonstrated that ammonium sulphate and sulphuric acid particles absorb light with low efficiency at the wavelength of the LDI laser used in our study. This observation was confirmed by results of a field campaign conducted in Atlanta (Georgia, USA), in which ammonium sulphate particles were substantially underestimated [Liu et al., 2003]. This effect is likely to have occurred also in our study and will be the subject of further work when the ATOFMS data are compared with a simultaneously run MOUDI impactor (Dall'Osto et al., manuscript in preparation, 2004).

[48] A considerable proportion of the acid generated in the atmosphere by oxidation of sulphur dioxide and nitrogen oxides is neutralized by NH3. As a result, ammonium is a major component of atmospheric aerosols [Asman et al., 1998]. The criterion used for searching ammonium-containing particles was the presence of signal at m/z 18 ([NH4]+). In ATOFMS positive ion spectra, the presence of particulate H2O is typically indicated by a peak at m/z 19 [H3O]+ [Noble and Prather, 1996], and therefore it does not interfere with the ammonium marker used. In our study, 5.2% of particles were classified as containing ammonium, and these were highly associated with sulphate, both in fine (85%) and coarse mode (83%) particles. Coarse ammonium was found to be associated also with nitrate mainly within dust-type particles.

4. Conclusion

[49] By using an aerosol time-of-flight mass spectrometer, different sources of aerosols were determined and apportioned at Mace Head (Ireland) during August 2002. Detailed information on qualitative chemical composition and particle size distributions were derived at high time resolution. The major particle types at Mace Head were classified as sea salt, soil dust, and carbon-containing particles. Detailed analysis of major particle types showed variable degrees of mixing of different secondary species including organic carbon, sulphate, nitrate, and ammonium. The major particle class was sea salt, which was subdivided according to the degree of replacement of chloride by nitrate. Two types of dust particles were found, both occurring mainly in the coarse mode (>1 μm): one type, postulated as originating from the Sahara, was characterized by an aluminium/silicon signature, while the other type, with a more local origin, was characterized by a Ca-rich composition. Dust-type particles contained peaks due to lithium, sodium, potassium, titanium, and iron as well as secondary species. Carbon-containing particles were mainly distributed in the fine mode (<1 μm) and were highly correlated with episodes of air pollution, either from mainland Europe or North America. Various metals were associated with carbon-

containing particles in different size modes, suggesting different mechanisms of formation and different origins.

Acknowledgments

[50] The authors are grateful to the Natural Environment Research Council for funding this work as part of the NAMBLEX consortium project coordinated by Dwayne Heard of the University of Leeds. They also thank John Methven (University of Reading) for back trajectories, Darius Cebernius (Galway University) for sampling dust at Mace Head, and Emily Norton (Aberystwyth University) for meteorological data. We are also grateful to the two reviewers for many suggestions that have improved the quality of this paper.

References

Allen, J. O., D. P. Fergenson, E. E. Gard, L. S. Hughes, B. D. Morrical, M. J. Kleeman, D. S. Gross, M. E. Galli, K. A. Prather, and G. R. Cass (2000), Particle detection efficiencies of aerosol time of flight mass spectrometers under ambient sampling conditions, Environ. Sci. Technol., 34(1), 211–217.

Arimoto, R., R. A. Duce, B. J. Ray, W. G. Ellis, J. D. Cullen, and J. T. Merrill (1995), Trace-elements in the atmosphere over the North Atlantic, J. Geophys. Res., 100(D1), 1199–1213.

Asman, W. A. H., M. A. Sutton, and J. K. Schjorring (1998), Ammonia: Emission, atmospheric transport and deposition, New Phytol., 139(1), 27–48.

Bergametti, G., L. Gomes, G. Coude-Gaussen, P. Rognon, and M. N. Le Coustumer (1989), African dust observed over Canary Islands: Source-regions identification and transport pattern for some summer situations, J. Geophys. Res., 94(D12), 14,855–14,864.

Bhave, P. V., M. J. Kleeman, J. O. Allen, and L. S. Hughes (2002), Evaluation of an air quality model for the size and composition of source-oriented particle classes, Environ. Sci. Technol., 36(10), 2154–2163.

Cape, J. N., J. Methven, and L. E. Hudson (2000), The use of trajectory cluster analysis to interpret trace gas measurements at Mace Head, Ireland, Atmos. Environ., 34(22), 3651–3663.

Castro, L. M., C. A. Pio, R. M. Harrison, and D. J. T. Smith (1999), Carbonaceous aerosol in urban and rural European atmospheres: Estimation of secondary organic carbon concentrations, Atmos. Environ., 33(17), 2771–2781.

Chester, R., E. J. Sharples, G. S. Sanders, and A. C. Saydam (1984), Saharan dust incursion over the Tyrrhenian Sea, Atmos. Environ., 18(5), 929–935.

Cooke, W. F., S. G. Jennings, and T. G. Spain (1997), Black carbon measurements at Mace Head, 1989–1996, J. Geophys. Res., 102(D21), 25,339–25,346.

Gard, E., J. E. Mayer, B. D. Morrical, T. Dienes, D. P. Fergenson, and K. A. Prather (1997), Real-time analysis of individual atmospheric aerosol particles: Design and performance of a portable ATOFMS, Anal. Chem., 69(20), 4083–4091.

Gard, E. E., et al. (1998), Direct observation of heterogeneous chemistry in the atmosphere, Science, 279(5354), 1184–1187.

Goudie, A. S., and N. J. Middleton (2001), Saharan dust storms: Nature and consequences, Earth Sci. Rev., 56(1–4), 179–204.

Gross, D. S., M. E. Galli, P. J. Silva, and K. A. Prather (2000), Relative sensitivity factors for alkali metal and ammonium cations in single particle aerosol time-of-flight mass spectra, Anal. Chem., 72(2), 416–422.

Harrison, R. M., and C. A. Pio (1983), Size-differentiated composition of inorganic atmospheric aerosols of both marine and polluted continental origin, Atmos. Environ., 17(9), 1733–1738.

Harrison, R. M., M. I. Msibi, A. M. N. Kitto, and S. Yamulki (1994), Atmospheric chemical-transformations of nitrogen-compounds measured in the North-Sea experiment, September 1991, Atmos. Environ., 28(9), 1593–1599.

Harrison, R. M., et al. (Eds.) (1999), Source Apportionment of Airborne Particulate Matter in the United Kingdom: The First Report of the Airborne Particles Expert Group, Dep. of the Environ., Transp. and Reg., London.

Heintzenberg, J., D. C. Covert, and R. Van Dingenen (2000), Size distribution and chemical composition of marine aerosols: A compilation and review, Tellus, Ser. B, 52(4), 1104–1122.

Huang, S., R. Arimoto, and K. A. Rahn (2001), Sources and source variations for aerosol at Mace Head, Ireland, Atmos. Environ., 35(8), 1421–1437.

Jennings, S. G., F. M. McGovern, and W. F. Cooke (1993), Carbon mass concentration measurements at Mace Head, on the west-coast of Ireland, Atmos. Environ. Part A, 27(8), 1229–1239.

Jennings, S. G., M. Geever, F. M. McGovern, J. Francis, T. G. Spain, and T. Donaghy (1997), Microphysical and physico-chemical characterization of atmospheric marine and continental aerosol at Mace Head, Atmos. Environ., 31(17), 2795–2808.

Kerminen, V. M., K. Teinila, R. Hillamo, and T. Pakkanen (1998), Substitution of chloride in sea-salt particles by inorganic and organic anions, J. Aerosol Sci., 29(8), 929–942.

Kleefeld, S., A. Hoffer, Z. Krivacsy, and S. G. Jennings (2002), Importance of organic and black carbon in atmospheric aerosols at Mace Head, on the west coast of Ireland (53°19′N, 9°54′W), Atmos. Environ., 36(28), 4479–4490.

Liu, D. Y., K. A. Prather, and S. V. Hering (2000), Variations in the size and chemical composition of nitrate-containing particles in Riverside, CA, Aerosol Sci. Technol., 33(1–2), 71–86.

Liu, D.-Y., R. J. Wenzel, and K. A. Prather (2003), Aerosol time-of-flight mass spectrometry during the Atlanta Supersite Experiment: 1. Measurements, J. Geophys. Res., 108(D7), 8426, doi:10.1029/2001JD001562.

Monn, C., O. Braendli, G. Schaeppi, C. Schindler, U. Ackerman-Liebrich, P. Leuenberger, and SAPALDIA team (1995), Particulate matter <10 μm (PM10) and total suspended particulates (TSP) in urban, rural and alpine air in Switzerland, Atmos. Environ., 29(19), 2565–2573.

Morales, C. (1986), The airborne transport of Saharan dust—A review, Clim. Change, 9(1–2), 219–241.

Moskalyk, R. R., and A. M. Alfantazi (2003), Processing of vanadium: A review, Miner. Eng., 16(9), 793–805.

Neubauer, K. R., M. V. Johnston, and A. S. Wexler (1997), On-line analysis of aqueous aerosols by laser desorption ionization, Int. J. Mass Spectrom. Ion Processes, 163(1–2), 29–37.

Neubauer, K. R., M. V. Johnston, and A. S. Wexler (1998), Humidity effects on the mass spectra of single aerosol particles, Atmos. Environ., 32(14–15), 2521–2529.

Noble, C. A., and K. A. Prather (1996), Real-time measurement of correlated size and composition profiles of individual atmospheric aerosol particles, Environ. Sci. Technol., 30(9), 2667–2680.

Noble, C. A., and K. A. Prather (1998), Single particle characterization of albuterol metered dose inhaler aerosol in near real-time, Aerosol Sci. Technol., 29(4), 294–306.

O'Dowd, C. D., et al. (2002), A dedicated study of New Particle Formation and Fate in the Coastal Environment (PARFORCE): Overview of objectives and achievements, J. Geophys. Res., 107(D19), 8108, doi:10.1029/2001JD000555.

Pakkanen, T. A. (1996), Study of formation of coarse particle nitrate aerosol, Atmos. Environ., 30(14), 2475–2482.

Pastor, S. H., J. O. Allen, L. S. Hughes, P. Bhave, G. R. Cass, and K. A. Prather (2003), Ambient single particle analysis in Riverside, California by aerosol time-of-flight mass spectrometry during the SCOS97-NARSTO, Atmos. Environ., 37(2), 239–258.

Poledniok, J., and F. Buhl (2003), Speciation of vanadium in soil, Talanta, 59(1), 1–8.

Prather, K. A., T. Nordmeyer, and K. Salt (1994), Real-time characterization of individual aerosol-particles using time-of-flight mass-spectrometry, Anal. Chem., 66(9), 1403–1407.

Raes, F., R. Van Dingenen, E. Vignati, J. Wilson, J. P. Putaud, J. H. Seinfeld, and P. Adams (2000), Formation and cycling of aerosols in the global troposphere, Atmos. Environ., 34(25), 4215–4240.

Rajkumar, W. S., and A. S. Chang (2000), Suspended particulate matter concentrations along the East-West Corridor, Trinidad, West Indies, Atmos. Environ., 34(8), 1181–1187.

Rodriguez, S., X. Querol, A. Alastuey, G. Kallos, and O. Kakaliagou (2001), Saharan dust contributions to PM10 and TSP levels in southern and eastern Spain, Atmos. Environ., 35(14), 2433–2447.

Roth, B., and K. Okada (1998), On the modification of sea-salt particles in the coastal atmosphere, Atmos. Environ., 32(9), 1555–1569.

Ryall, D. B., R. G. Derwent, A. J. Manning, A. L. Redington, J. Corden, W. Millington, P. G. Simmonds, S. O'Doherty, N. Carslaw, and G. W. Fuller (2002), The origin of high particulate concentrations over the United Kingdom, March 2000, Atmos. Environ., 36(8), 1363–1378.

Savoie, D. L., R. Arimoto, W. C. Keene, J. M. Prospero, R. A. Duce, and J. N. Galloway (2002), Marine biogenic and anthropogenic contributions to non-sea-salt sulfate in the marine boundary layer over the North Atlantic Ocean, J. Geophys. Res., 107(D18), 4356, doi:10.1029/2001JD000970.

Silva, P. J., and K. A. Prather (2000), Interpretation of mass spectra from organic compounds in aerosol time-of-flight mass spectrometry, Anal. Chem., 72(15), 3553–3562.

Silva, P. J., D. Y. Liu, C. A. Noble, and K. A. Prather (1999), Size and chemical characterization of individual particles resulting from biomass burning of local southern California species, Environ. Sci. Technol., 33(18), 3068–3076.

Silva, P. J., R. A. Carlin, and K. A. Prather (2000), Single particle analysis of suspended soil dust from southern California, Atmos. Environ., 34(11), 1811–1820.

Song, X. H., P. K. Hopke, D. P. Fergenson, and K. A. Prather (1999), Classification of single particles analyzed by ATOFMS using an artificial neural network, ART-2A, Anal. Chem., 71(4), 860–865.

Thomson, D. S., A. M. Middlebrook, and D. M. Murphy (1997), Thresholds for laser-induced ion formation from aerosols in a vacuum using ultraviolet and vacuum-ultraviolet laser wavelengths, Aerosol Sci. Technol., 26(6), 544–559.

Vitolo, S., M. Seggiani, S. Filippi, and C. Brocchini (2000), Recovery of vanadium from heavy oil and Orimulsion fly ashes, Hydrometallurgy, 57(2), 141–149.

Wenzel, R. J., D.-Y. Liu, E. S. Edgerton, and K. A. Prather (2003), Aerosol time-of-flight mass spectrometry during the Atlanta Supersite Experiment: 2. Scaling procedures, J. Geophys. Res., 108(D7), 8427, doi:10.1029/2001JD001563.

Yeatman, S. G., L. J. Spokes, and T. D. Jickells (2001), Comparisons of coarse-mode aerosol nitrate and ammonium at two polluted coastal sites, Atmos. Environ., 35(7), 1321–1335.

Zhang, D. X., and R. G. Cooks (2000), Doubly charged cluster ions (NaCl)(m)(Na)(2)(2+): Magic numbers, dissociation, and structure, Int. J. Mass Spectrom., 196, 667–684.

Zhuang, H., C. K. Chan, M. Fang, and A. S. Wexler (1999), Formation of nitrate and non-sea-salt sulfate on coarse particles, Atmos. Environ., 33(26), 4223–4233.